NEGATIVE OBSTACLE SENSING BASED ON REAL DATA OF ULTRA-WIDEBAND SAR

Zhibiao Jiang[1], Jian Wang[1], Qian Song[1] , Zhimin Zhou[1]

[1]*College of Electronic Science and Engineering, National University of Defense Technology*
Changsha, Hunan, P.R. China，410073
13596458441@163.com

Keywords: Negative obstacle, unmanned ground vehicle, unstructured environments, ultra-wideband, synthetic aperture radar (SAR).

Abstract

It is a difficult task for an unmanned ground vehicle using regular sensor to sense obstacles in unstructured environments or out fields, especially on negative obstacle sensing. In this paper, we present an approach for negative obstacle sensing, based on ultra-wideband synthetic aperture radar (SAR) image characteristic of negative obstacle sensing. And real data on negative obstacle sensing is collected by ultra-wideband synthetic aperture radar (SAR). In all, we carried out three experiments by using three different frequency band antennas, and experimental results show that ultra-wideband synthetic aperture radar (SAR) can display edge information of negative obstacle in synthetic aperture radar (SAR) images.

1 Introduction

Autonomous off-road navigation is important in applications of unmanned ground vehicles in agriculture, defense, and planetary exploration. However, a key open problem for UGV perception is sensing obstacles, and the most challenge part is sensing negative obstacles. Most prior research on negative obstacle sensing has been done by the small community working on autonomous off-road navigation, and the main sensors used to sensing obstacles are stereo cameras [1,2,3,4], infrared detectors [5,6] and ladar [7,8,9]. The authors G. Witus and R. Karlsen [1], use stereo cameras they rely on shadows cast by negative obstacle. Those shadows cast by negative obstacle provide cues to complement and enhance stereo vision. The authors Matthies and Rankin[5] show that the interiors of negative obstacle generally remain warmer than the surrounding terrain throughout the night, making thermal signature a stable property for night-time negative obstacle detection.Existing techniques use three-dimensional ladar data, as in [8]. The authors present an approach for potential negative obstacle detection, based on missing data interpretation that extends traditional techniques driven by data only, which capture the occupancy of the scene. They have already done a good job on sensing obstacles in constructed environments, but they has not, to our knowledge, led to successful or published results on negative obstacle sensing in unstructured environments or out fields.

Nowadays, it's acknowledged that ultra-wideband synthetic aperture radar combine ultra-wideband advanced technique with synthetic aperture advanced technique together. Ultra-wideband synthetic aperture radar (SAR) is not only have the ability to work on high resolution in a broad range of environments and weather conditions, but also have advantage on penetrating ground vegetation, wide angle of view, quick scanning etc, which make ultra-wideband SAR a promising method for sensing negative obstacles. It's becoming a hot research on environment senses of unmanned ground vehicle [10].

In this paper, we seek to use ultra-wideband synthetic aperture radar (SAR) to detect negative obstacle, and try to find obstacle feature from the high resolution image. Our approach has several advantages over other pre-existing approaches to detect negative obstacle. First, the approach has potential ability to detect negative obstacle in foliage (such as tall grass), because our sensor can penetrate ground vegetation. Second, since our sensor can work in all weather, day/night at large standoff distances, so the approach has sound commonality. Finally, the approach has mature technological base.

There are different kinds of negative obstacle in actual environments, in brief saying, negative obstacle could be classified into their three types: cliff type, negative step type and ditch type, as are shown in Fig. 1. The thick part lines mean the invisible portion of negative obstacles. In this paper, ditch type of negative obstacle was taken for example.

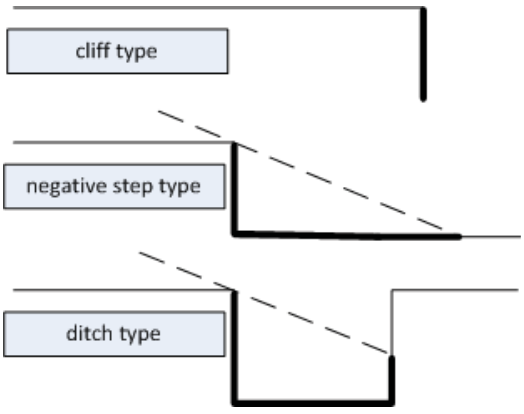

Fig. 1: Types of negative obstacles

An outline of the paper is as follows. First, we state the SAR echo signal model, for phase history data collection and image formation. Second, we describe back projection (BP) algorithm. Then, we carried out experiments for negative obstacle sensing. Finally, we state our conclusions and outline areas of future work.

2 SAR echo signal model

Ultra-wideband SAR makes use of wideband to obtain high range resolution, and make use of long synthetic aperture to acquire high azimuth resolution. It's also foundation of two dimensions imaging.

Taking the strip map SAR for example, since the SAR image is synthesized by the data from the antenna at different positions along the path as shown in Fig. 2, where r, y denote the slant range and azimuth position respectively, r-y the imaging plane. The height of radar apart from ground is H, and Radar move with uniform speed along the direction of y axis. T is one of target in imaging scene.

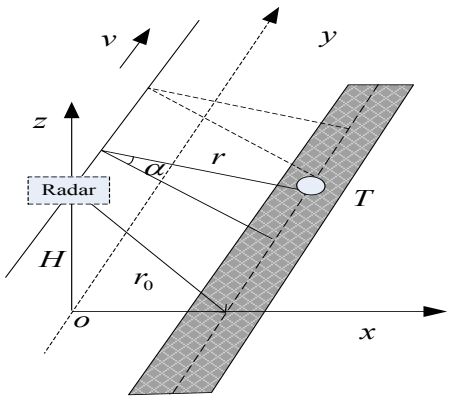

Fig. 2: Geometry model of SAR imaging

According to geometrical relationship show in Fig. 2, the instant range of the target to radar is

$$r = \sqrt{\left(vt_a - y_T\right)^2 + r_0^2} \tag{1}$$

The SAR system use stepped frequency waveform as transmit signal. The stepped frequency waveform uses a sequence of pulses to achieve ultra-wide bandwidth, where each pulse has a single frequency. We denote the transmitted waveform as

$$s_t\left(n,\tau\right) = rect\left(\tau / T_{pn}\right)\exp\left(j2\pi f_c\left(n\right)\tau\right) \tag{2}$$

Where $n = 1, 2\cdots, N$ denotes the nth pulse in a sequence, N is the number of pulses in one sequence, τ is the signal time, $rect\left(\tau / T_{pn}\right)$ denotes a rectangular window, T_{pn} is the window width, and $f_c\left(n\right)$ is the center frequency of the nth pulse.

For a point reflector at range r, neglecting the reflection coefficient, the echo is

$$s_r\left(n,\tau\right) = rect\left(\frac{\tau\text{-}2r/c}{T_{pn}}\right)\exp\left(j2\pi f_c\left(n\right)\left(\tau\text{-}2r/c\right)\right) \tag{3}$$

Where c is the velocity of light, $f_c\left(n\right) = f_c + n\Delta f$, $n = 1, 2\cdots, N$,where f_c is the start frequency and Δf is the frequency step length.

3 Imaging algorithm

Back projection (BP) algorithm is commonly used in unmanned ground vehicle for its high image quality and being compensated easily. In back-projection method, each received radar echo is processed and back-projected over spherical shells to all imaged ground pixels. Then, each pixel is thus assigned a value by interpolating the pulse echo at the time delay which is corresponding to the range between the pixel and the antenna. The values for each pixel are accumulated as more radar echoes are processed until all echoes have been processed and the final resolution achieved. BP algorithm is performed in the time-domain (or echo domain), and thus it is easier to be integrated with motion compensation than those frequency-domain image formations [11].

The conventional 2-D BP algorithm [12] could be formulated by(4).

$$f\left(x,r\right) = \iint \frac{t^2}{r} d\left(\hat{\mathrm{x}},t\right) w\left(\frac{\hat{\mathrm{x}}\text{-}x}{r}\right)\delta\left(t - \frac{2R\left(x,r,\hat{\mathrm{x}}\right)}{c}\right) d\hat{\mathrm{x}}dt \tag{5}$$

Where $d\left(\hat{\mathrm{x}},t\right)$ is the raw data, $\hat{\mathrm{x}}$ is the radar position, $w\left(\frac{\hat{\mathrm{x}}\text{-}x}{r}\right)$ denote shape function of the antenna. $R\left(x,r,\hat{\mathrm{x}}\right)$ is the distance between radar and the point to image, whose coordinates are $\left(\hat{\mathrm{x}},t\right)$.

4 Experiments

We carried out experiments for negative obstacle SAR imaging. Our SAR system is a mono-static radar system, which employ a single platform operating as both transmitter and receiver, and generate two-dimensional (2D) SAR images generated from linear paths. The ultra-wideband SAR was mounted on a rail to collect data. The rail is controlled by a micro-computer, and the ultra-wideband SAR can move on the rail with a preset velocity. Fig. 3 shows the principle diagram of ultra-wideband SAR system.

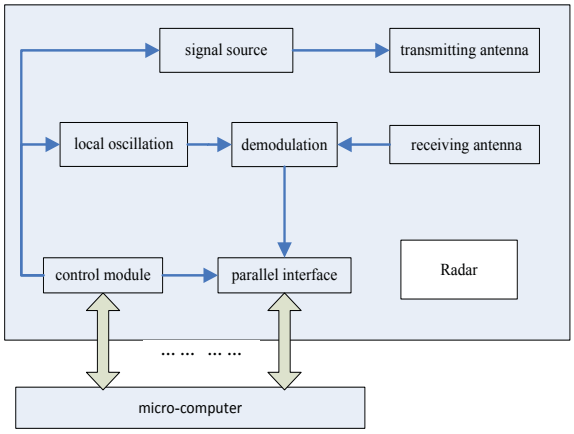

Fig. 3: The principle diagram of SAR system

Fig. 4 shows the photograph of ultra-wideband SAR system in experimental scene, the radar mounted on the rail, and Fig. 5 shows the experiment ground, the target is a man-made ditch type of negative obstacle. The ultra-wideband SAR system use stepped frequency waveform.

Fig. 4: Experimental scene

Fig. 5: A ditch type of negative obstacles

We have conducted three experiments by using three different frequency band antennas. Fig. 6 shows the antennas. The biggest antenna in Fig. 6 is used for transmitting and receiving signal which frequency band is 6-8GHz. The middle antenna in Fig. 6 is used for transmitting and receiving signal which frequency band is 9-11GHz. The smallest antenna in Fig. 6 is used for transmitting and receiving signal which frequency band is 13-15GHz.

Fig. 6: Three different frequency band antennas

In the first experiment, Radar velocity is 0.05m/s, Radar moving distance on the rail is 1.2m. The height of radar apart from ground is 1.45m.The signal frequency band is 6-8GHz. Frequency step is 4MHz.The frequency number is 501.
The imaging area is (range position: 4~15m)*(azimuth position: -3~3m).The imaging pixel interval along range direction is 0.05m. The imaging pixel interval along azimuth direction is 0.05m. According to BP algorithm, the imaging result is shown in Fig. 7.

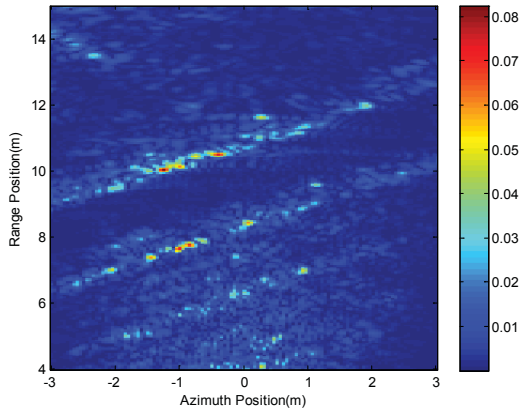

(a) Two-dimensional (2D) SAR image

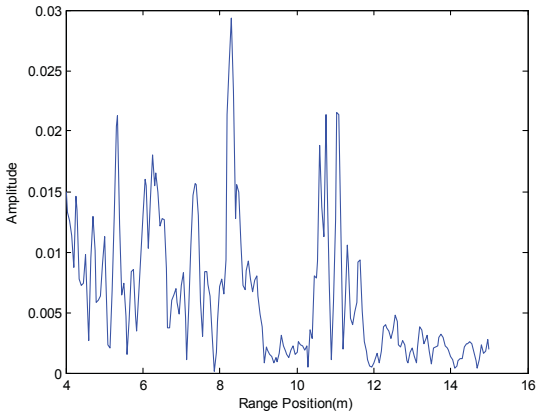

(b)Range profile at zero azimuth position

Fig. 7: Imaging results

Fig. 7(a) shows the two-dimensional (2D) SAR image of negative obstacle sensing. From the SAR image, we can see two bright lines, which have the similar shape with the edge of the ditch type of negative obstacle. Fig. 7(b) is the range profile of the two-dimensional (2D) SAR image at zero azimuth position.
In the second experiment, Radar velocity is 0.05m/s, Radar moving distance on the rail is 1.2m. The height of radar apart from ground is 1.45m.The signal frequency band is 9-11GHz. Frequency step is 4MHz. The frequency number is 501.
The imaging area is (range position: 4~15m)*(azimuth position: -3~3m). The imaging pixel interval along range direction is 0.05m. The imaging pixel interval along azimuth direction is 0.05m. According to BP algorithm, the imaging result is shown in Fig. 8.

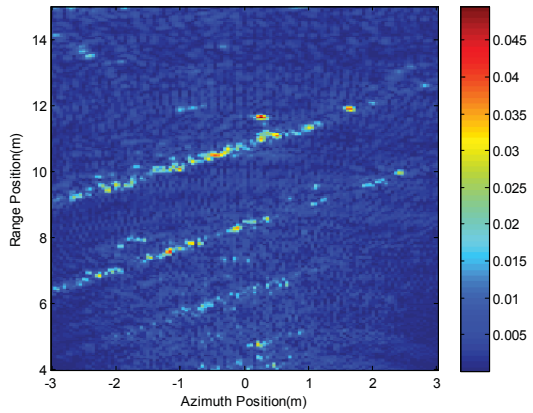

(a) Two-dimensional (2D) SAR image

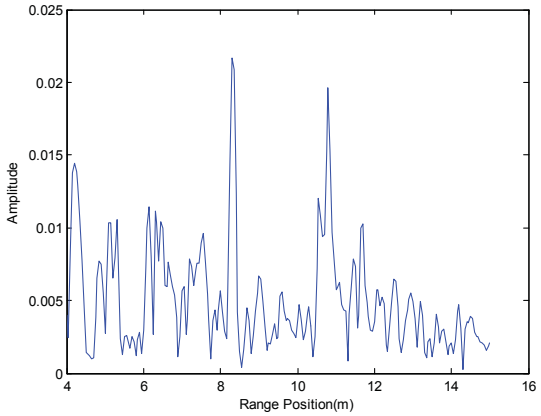

(b) Range profile at zero azimuth position

Fig. 8: Imaging results

Fig. 8(a) shows the similar result with Fig. 7(a). From the SAR image, we can see two bright lines, which have the similar shape with the edge of the ditch type of negative obstacle. Fig. 8(b) is the range profile of the two-dimensional (2D) SAR image at zero azimuth position.

In the third experiment , Radar velocity is 0.05m/s, Radar moving distance on the rail is 1.2m. The height of radar apart from ground is 1.45m.The signal frequency band is 13-15GHz. Frequency step is 4MHz. The frequency number is 501.

The imaging area is (range position: 4~15m)*(azimuth position: -3~3m). The imaging pixel interval along range direction is 0.03m. The imaging pixel interval along azimuth direction is 0.03m. According to BP algorithm, the imaging result is shown in Fig. 9.

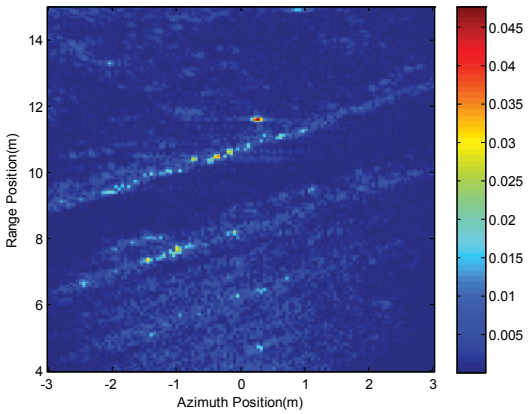

(a) Two-dimensional (2D) SAR image

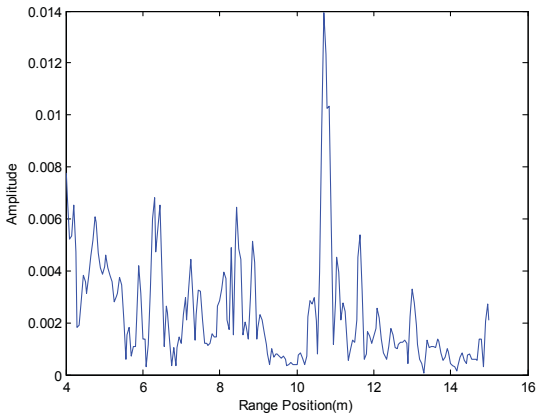

(b) Range profile at zero azimuth position

Fig. 9: Imaging results

From the SAR image Fig. 9(a), we can also see two lines although one of lines is ambiguity, which have the similar shape with the edge of the ditch type of negative obstacle. Fig. 8(b) is the range profile of the two-dimensional SAR image at zero azimuth position.

By comparing the SAR image results of three frequency band 6-8GHz、9-11GHz、 13-15GHz, major conclusions are as follows. First, ultra-wideband SAR can show the edge information of the ditch type of negative obstacle in the two-dimensional SAR image. Second, there are ground clutter and noise existing in SAR image .If we reduce levels of ground clutter and noise, we could make the edge of the ditch type of negative obstacle more clearly in the two-dimensional SAR image. Finally, the coherent speckle still exists in SAR images of three frequency band. The effective measures should be taken to suppress the coherent speckle in SAR image for reducing the effect of speckle on classification and detection if necessary.

5 Conclusions

Negative obstacle sensing is a very challenging problem .In this paper, we presented an original approach for negative obstacle sensing by using ultra-wideband SAR. In order to

find obstacle features from the high resolution SAR images, we carried out experiment for negative obstacle sensing. From the SAR image that the signal frequency band is 6-8GHz, we find out that ultra-wideband SAR can show the edge information of the ditch type of negative obstacle. In an attempt to make sure the image feature of negative obstacle, we also carried out experiments for negative obstacle sensing that the signal frequency band is 9-11GHz、13-15GHz, and we find out the same result. Future work will necessarily involve further development of this approach. One might also further study the coherent speckle reduction in SAR image of negative obstacle and the SAR image characteristics extraction for negative obstacle classification and detection.

Acknowledgements

This work was supported in part by 1) and 2).

1) The National Natural Science Foundation of China under Grant 61271441

2) Research Project of National University of Defense Technology under Grant CJ12-04-02.

References

[1] G. Witus, R. Karlsen, D. Gorsich, and G. Gerhart, “Preliminary investigation into the use of stereo illumination to enhance mobile robot terrain perception,” in Unmanned Ground Vehicle Technology III, 2001.

[2] A. Rankin, A. Huertas, L. Matthies. “Evaluation of Stereo Vision Obstacle Detection Algorithms for Off-road Autonomous Navigation”, AUVSI's Unmanned Systems North America, 2005, pp.1197-1211.

[3] P. Bellutta, R. Manduchi, L Matthies, K. Owens, “A. Rankin. Terrain Perception for DEMO III”. IEEE Intelligent Vehicles Symposium, 2000, pp. 326–331.

[4] C. Caraffi, S. Cattani, and P. Grisleri. “Off-road Path and Obstacle Detection using Decision Networks and Stereo Vision”, IEEE Transactions on Intelligent Transportation, 2007, 8, (4), pp. 607-618.

[5] L. Matthies, A. Rankin. “Negative Obstacle Detection by Thermal Signature”, IEEE International Conference on Intelligent Robots and Systems, 2003, pp.906-913.

[6] A. Rankin, A. Huertas, L. Matthies. “Nighttime Negative Obstacle Detection for Off-road Autonomous Navigation”, Proceedings of the International Conference on Intelligent Robots and Systems, 2007, pp. 906-913.

[7] J.-F. Lalonde, N. Vandapel, M. Huber, and M. Hebert, “Natural terrain classification using three-dimensional ladar data for ground robot mobility,” Journal of Field Robotics, 2006,23,(10),839-861.

[8] N. Heckman, J. Lalonde, N. Vandapel and M. Hebert. “Potential Negative Obstacle Detection by Occlusion Labeling”, Proceedings of the IEEE Conference on Intelligent Robots and Systems, 2007, pp. 2168-2173.

[9] Albert Diosi and Lindsay Kleeman. “Uncertainty of Line Segments Extracted from Static SICK PLS Laser Scans”, Proceedings of Australasian Conference on Robotics and Automation，2003.

[10] Song Jun Park, James A. Ross, “Hybrid Core Acceleration of UWB SIRE Radar Signal Processing”, IEEE Trans. on Parallel and Distributed System , 2011, 22, (1), pp. 46-57.

[11] Tian Jin, Zhimin Zhou, Wenge Chang, “Ultra-wideband SAR time-frequency representation image formation”, IEE Proceedings: Radar, Sonar and Navigation, 2006, 153, (5), pp. 389-395.

[12] Richard Rau, James H.Mcclellan. “Analytic Models and Post processing Techniques for UWB SAR”, IEEE Trans on AES, 2000, 36,(4) , pp. 1058-1074.